*

Evolution and complexity of the seismogenic Düzce fault zone (Turkey) depicted by coseismic ruptures, Plio-Quaternary structural pattern and geomorphology

S. Pucci [a,b,*], D. Pantosti [a], M.R. Barchi [b], N. Palyvos [a]

[a] *Istituto Nazionale di Geofisica e Vulcanologia, Via di Vigna Murata 605, 00143 Rome, Italy*

[b] *Dipartimento di Scienze della Terra, Università degli studi di Perugia,Piazza Università, 06123 Perugia, Italy*

* Corresponding author. Current address: *Istituto Nazionale di Geofisica e Vulcanologia, Via di Vigna Murata 605, 00143 Rome, Italy* , Tel.: +39-6-51860406, Fax: +39-6-51860507.

E-mail address: pucci@ingv.it (S. Pucci).

***Keywords*:** Coseismic ruptures; Tectonic geomorphology; Slip distribution; Releasing fault junction; Dislocation model; 1999 Düzce earthquake.

Abstract

We investigated the area struck by the November, 12, 1999, Mw 7.1 earthquake that ruptured the Düzce segment of the North Anatolian Fault Zone (NAFZ) three months after the August, 17, 1999, Mw 7.4 Izmit earthquake. On the basis of 1:25.000 scale field survey and aerial photo interpretation we identified a simple 1999 coseismic fault trace (CFT) and an older complex fault system (PQFS), involving a wider zone of deformation.

Overall, we recognized two different sections of the Düzce segment: a western section, where the coseismic fault trace has a staircase trajectory and reactivated part of the older fault system; an eastern section, where the coseismic fault trace shows a straight trajectory and cross-cuts the older and complex fault system. The Düzce fault sections may represent different stages of the segment evolution. In fact, the collected data suggest the tendency of the fault to simplify its trace with time and to evolve from a complex towards a simpler mature trace, as a mechanically more favorable setting.

The western section of the Düzce fault segment splays out from a restraining bend of the Izmit (Karadere) fault segment of the NAFZ, and forms a releasing fault wedge. By comparing the coseismic surface deformation field with the observed long-term morphology it is clear that the present landforms and setting are the result of 1999-type coseismic deformation repeating through several seismic cycles. Because of the mechanical interaction of the faults in the release junction, the western section of the Düzce fault undergoes a lower normal stress that may justify its complexities and earlier stage of evolution at the surface.

The boundary at the surface between the two portions of the Duzce fault is not only a surface characteristic but it separates at depth a portion of fault plane characterized by a

big single asperity, to the east, from a portion of plane with lower slip, to the west. Thus the peculiar arrangement of the Izmit (Karadere) and Düzce fault segments may permanently control the difference in behavior of the two portions of Duzce fault and furthermore control rupture propagation and fault loading. Under this light, the Izmit/Düzce release fault junction (1) may produce an unfavorable setting for the build up of asperities in the western part of the Düzce segment also in the future and (2) could have delayed the propagation of the 1999 August Izmit rupture on the Düzce segment that ruptured on November 1999 along the asperity of its eastern section.

These results highlight that the surface geological data contain the potential for integrating and completing the information for imaging structures also at a seismogenic depth.

1. Introduction

In regions of high active strain, the long-term effects of active faulting on landscape and geological structures are outstanding. The occurrence of repeated coseismic deformation, that accumulates during time, controls the growth and development of both geological and morphological structures. Thus, the landscape and structural setting of active regions contain the long-term record of the active faults behavior. The study of the features representing these long-term records can be compared with the coseismic evidence (as derived from geological -e.g. surface ruptures- or seismological data) in order to unequivocally determine the present-day active fault setting and consequently get information on complexities and evolution of the fault during time. This type of information is critical in the study of seismogenic faults, in particular for the recognition of the persistency of fault surface boundaries or fault internal complexity. The importance of defining a persistent fault boundary at the surface derives from the fact that such discontinuities might match and illuminate discontinuities of the seismogenic source that control its rupture behaviour at depth and that may have a strong impact on the rupture propagation (*i.e.*, earthquake size) [1-6 and reference therein].

Along the active transform margin of North Anatolia, the prominent geomorphic signature of the strike slip faulting is one of the main direct consequences of the longlasting (Late Miocene-Early Pliocene to present [7, 8]) and relevant present strain (20-30 mm/yr by means of GPS data [9-14]; from 5 to 18 mm/yr by means of geological data; [7, 15-18]). Several repeated surface-rupturing earthquakes along the North Anatolian Fault are known to contribute to the build up of this long-term geomorphic signature [3, 19-21]. One of these earthquakes, that occurred on November 12, 1999 along the Düzce fault segment, produced surface ruptures that are still well-preserved along a 40 km-long mountain front, that also shows good evidence of its long-term tectonic history. This makes

the Düzce fault a natural laboratory where coseismic deformation, long-term landforms and geological structures can be studied and integrated in order to image the fault and its evolution.

Recent studies on the Düzce fault were mainly focused on the coseismic ruptures and slip distribution (eg. [22, 23]). In this work we developed an integrated study of the coseismic features and long-term evidence of fault activity as recorded in the geology and landscape in a broad area around the fault. We also used elastic dislocation modeling in order to better understand if the present landform is the result of accumulation of 1999-type deformation repeated through several seismic cycles. Finally, to investigate the consistency of the surficial long-term fault expression with the deep coseismic fault behavior, we compared the shallow fault complexities obtained from surface mapping with the slip distribution at depth modeled by Delouis et al. [24].

2. The 1999 earthquake on the Düzce fault segment of the North Anatolian Fault Zone (NAFZ)

The NAFZ is an active right-lateral system, about 1500 km long, which bounds to the north the westward-extruding Anatolian block [7, 8; 25-28] (see inset of figure 1). GPS networks measured present-day strain-rates of 20-30 mm/yr [9-14] in the northern part of the Anatolian block, with vectors oriented WNW in the easternmost region, E-W in the centre, and SW in the Aegean. West of the town of Bolu, the North Anatolian Fault splays into two main strands, the Düzce fault to the north and the Mudurnu fault to the south (fig. 1). According to Ayhan et al. [29, 30], the Düzce fault accommodates up to 33% to 50% of the present-day GPS strain across the NAFZ (ca. 10 mm/yr).

The present-day high strain rate of the NAFZ is seismically accommodated by a large number of earthquakes [19-21, 31-33; Harvard; USGS]. Following two large events that

ruptured two segments of the southern strand of the NAFZ along the Mudurnu valley in 1957 (Ms 7.0, [25]) and 1967 (Ms 7.1, [34, 35]), two highly damaging earthquakes occurred in 1999 along the northern strand (fig. 1). The first of these events (Mw 7.4, USGS) occurred on August 17 and struck the Izmit region, east of the Marmara Sea. It nucleated at a depth of 13 km and produced more than 150 km of surface ruptures organized in five major fault sections (fig. 1; Hersek, Karamursel-Golcuk, Izmit-Sapanca, Sapanca-Akyazi and Karadere sections; [36-38]), with dextral offsets exceeding 5 m. The second large event occurred three months later on November 12, 1999, and struck the Düzce area (Mw 7.1, USGS, KOERI). This was likely triggered by the previous event [39, 40]. The focal mechanism solution shows a ca. E-W nodal plane dipping 54° to 73° to the north, (Harvard CMT; USGS) (fig. 1). This earthquake nucleated at a depth of 10-15 km (CSEM, European-Mediterranean Seismological Centre; Tubitak, Marmara Research Centre) and produced ca. 40 km of surface ruptures, showing maximum dextral offset of 5 m (fig. 1) [22, 41]. Interestingly, the westernmost part of the Düzce fault segment slipped also during the August earthquake, but with only up to 25 cm horizontal and 10 cm vertical surface offset (fig. 1) [42, 43].

Modeled slip distribution at depth, obtained by different joint inversions (mostly teleseismic, strong motion, GPS and InSAR data, in some cases constrained by surface offsets) show consistently that the right-lateral Düzce rupture was simple and concentrated in space, with a single, round-shaped, 10-25 km-wide, 6-8 meters maximum slip asperity, located in the eastern part of the fault [24, 40, 44, 45].

3. The Düzce fault segment

The Düzce fault separates the Paleozoic-Eocene formations of the Almacik block from the Quaternary continental deposits of the Düzce basin (figs. 1 and 2), that was

interpreted by Aydin and Kalafat [46] as a composite pull-apart basin filled mainly with Pliocene deposits.

The eastern termination of the Düzce fault may join the eastern single trace of the NAFZ *via* a right-releasing step-over, formed by the WNW-ESE trending Bakacak and Elmalik faults (fig. 1). Conversely, the western part of the E-W trending Düzce fault splays out from the WSW-ENE trending Karadere section, that represents a restraining bend of the Izmit Fault. According to Lettis et al. [23], this western boundary of the Düzce fault segment forms a complex right releasing step-over with the Karadere section that presumably represented a barrier to the August rupture propagation. As a result, this releasing zone controls the present-day Düzce Basin depocentre, that coincides with Lake Efteni (fig. 2).

On the basis of its geometry, Akyuz et al. [22] subdivided the 1999 Düzce rupture into four sections. Each of them shows a symmetric slip tapering off at both ends and are separated by about 1-km wide releasing and restraining step-overs that, as would be expected for such small-scale features [3-6, 47, 48], did not represent in 1999 a barrier to the rupture propagation.

3.1. The1999 coseismic fault trace (CFT)

In order to analyze the relationships of Quaternary geological faulting with the 1999 earthquake ruptures collected new data and mapped in detail: a) structural patterns of fractures and faults; b) geomorphic modifications induced by the earthquake; c) coseismic offset of piercing points such as roads, fences, tree lines, channels, streams, buildings, etc. (fig. 2 and fig. 3).

The morphological expression of the 40 km-long CFT is predominantly *mole-track* type. In general, the mole-track structure is simple and narrow and forms a deformation zone 0.5 to 5 m-wide but occasionally becomes complex and its width increases up to 50

m. The deformation pattern of the CFT is typical of a complex dextral fault zone, consisting of associated, én-échelon rupture systems: a) left-stepping transtensional Riedel shears or T-shears; b) right-stepping transpressional P-shears; c) Y-shears, paralleling the mean strike of the rupture. This pattern is organized in over-stepping en-échelon systems, that can be recognized at different scales.

Even though the kinematics of the Düzce fault is dominantly strike-slip, field observations show the presence of widespread vertical motion also highlighted by InSAR data [44, 45]. The slip distribution curve (fig. 3), built by integrating the data collected by Akyuz et al. [22, 41] with more than 350 new measures, exhibit a large along strike variability, with 5.0 m maximum and 2.4 m average dextral offsets, and 2.5 m maximum vertical offset. Because the coseismic strike-slip is directly related to the movement along the seismogenic fault, the lower measured values, that cause such a great variability of the slip distribution, can be seen as a mechanical problem (i.e., bad connection between the rupture of the fault and the surface ruptures). If this is correct, the interpolation of the maximum values (fig. 3) describes the seismic moment at the surface. The coseismic dip-slip distribution is more complex, since many gravity effects and local transtensional or transpressional components can be involved.

The main characteristics of the slip distribution are: (1) the dextral coseismic offset of the CFT has a bow-shape, with slip tapering off at both ends (west of Efteni Lake and east of Kaynasli) whereas the central part has a constant and larger mean value of 2.7 m; (2) the vertical component of the western section of the CFT is higher than that of the eastern section; (3) the overall westernmost section produced uplift of the range front to the south, with respect to the plain to the north; (4), frequent change of dip-slip direction in the central part of the CFT; (5) the eastern part of the CFT produced relative subsidence of the northern block west of the Kaynasli basin and of the southern block east of it (fig. 2 and fig. 3).

The CFT does not continuously run at the mountain-piedmont junction, but crosses the mountain front and affects both basin infill deposits and bedrock. As a whole, the CFT can be divided into two main sections, joining close to the village of Cakirhaciibrahim (fig. 2). With respect to the mean E-W trend of the Düzce fault, the western section presents sharp changes in the strike direction, producing a saw-toothed trajectory, consisting of NE-SW and WNW-ESE trending elements. Moving to the Cakirhaciibrahim area, the saw-toothed setting leaves space to a simpler, E-W trending trace. Conversely, the eastern CFT shows a mainly rectilinear E-W trending trajectory, and contains two small, 1km-wide, left-steps, near Beykoy and west of Kaynasli (fig. 2).

The CFT is associated with a consistent pattern of landforms, indicating that the Düzce fault ruptured during repeated seismic cycles with similar location, geometry and kinematics (fig. 2). In fact, the CFT overprinted the long-term tectonic morphologies, such as pressure ridges, linear valleys, escarpments and flat irons that have been shaped on both Pleistocene-Holocene continental deposits and bedrock. However, there is a marked difference between the eastern E-W trending CFT, that exhibits more prominent landforms, and the few E-W trending portions of the western CFT, presenting weak long-term tectonic morphologies.

3.2. The Plio-Quaternary fault system (PQFS)

The analysis of the long-term geologic and geomorphic setting of the Düzce fault was performed extending the observation on a broader area around the CFT. We collected structural data and recognized morphotectonic elements that describe a long-term kilometric structural pattern, mainly consisting of én-échelon, left-stepping, WNW-ESE striking, Riedel shears and of right-stepping, SW-NE striking, P-shears (fig. 2).

The Riedel shears have a clear-cut geomorphologic expression and are confirmed by alignments of right-hand deflections of streams and suspended terraces at the stream

outlets. They can be, mostly, traced at the base of indented and roughly well preserved, up to 250 m high, facets (e.g., south of Efteni Lake, spot 1 in fig. 2), that eloquently depict their transtensive kinematics, or along well-aligned linear ridges, saddles and valleys (e.g., south of Beykoy, spot 2 in fig. 2). Three hot springs along two of the Riedel shears suggest that these are similarly rooted at depth.

The P-shears are characterized by SW-NE straight features (fig. 2), with an abrupt slope gradient change, evidence of important vertical movements, and strong stream incision. They do not have any litho-structural control and bedrock outcrops confirm the presence of similarly oriented fault planes. We could not identify clear kinematic indicators on these faults: we inferred their transpressive character on the basis of their orientation with respect to the Düzce fault stress field (see inset in fig. 2).

The activity of PQFS during the Plio-Quaternary deformational history of the Düzce fault is clearly expressed by its control on the sediment deposition (fig.2). Although with a different impact on the landforms, the combination of the NE-SW and WNW-ESE long-term fault systems of the PQFS developed the outstanding morphological features of the Düzce fault. Along the western section of the fault, the PQFS bounds the triangular embayments of the range front, that host bajadas filled by Middle-Late Pleistocene alluvial fan and Holocene fluvial deposits (spots a, b, and c in fig. 2), or also by Late Pliocene-Early Pleistocene conglomerate-sandstone units (spot d in fig. 2), shed from the southern highlands [49]. Another clear evidence of the control of the PQFS on the present geomorphology is provided by the Kaynasli lozenge-shaped basin located in the eastern part of the fault. Pull-apart opening and Late Pliocene-Holocene deposition in this basin has been controlled by two WNW-ESE main left-stepping Riedel shears that are part of the PQFS (fig. 2).

3.3. CFT versus PQFS

Given their characteristics and organization at the surface, both the PQFS and CFT may correspond to the complex surface expression of a “tulip” or “palm-tree” structure due pure strike-slip basement movement on a master fault at depth (i.e. Düzce seismogenic fault). Interestingly, this geometry has been also illuminated by trapped waves, in fact, analysis of anomalous features from the Düzce area seismograms shows a low-velocity layer interpreted as a kilometric-broad damage-zone, 3-4 km deep [52, 53].

The comparison of the CFT and the PQFS highlights that the Düzce Fault is composed of two parts with different settings: in the western part the CFT is strongly controlled by the PQFS setting, whereas, in the eastern part the CFT cuts across the PQFS features and assumes a quite linear independent trajectory. The western part of the CFT has a saw-tooth arrangement with changes of trajectory and *en échelon* left-stepping transtensive and right-stepping transpressive subsections with kinematics similar to the PQFS. This part contains also a few E-W trending elements (locations e, f and g in fig. 2), associated to subtle and youthful long-term landforms suggesting they have hosted a smaller cumulative deformation than the PQFS and may represent an incipient stage of evolution of the fault system from saw-tooth geometry to linear. Along this western part a small number of 1999 coseismic ruptures occurred along the traces of PQFS and suggest that part of the present-day slip is still accommodated by the PQFS (fig. 2).

Conversely, in the eastern part the CFT has completely overcome the PQFS and presents a more regular, E-W trajectory parallel to the mean trend of the seismogenic Düzce fault. The whole CFT eastern section is associated with a strong morphological imprint that indicates its persistent long-term activity. There is a marked difference between the eastern E-W trending CFT, that exhibits well developed landforms, and the few E-W trending portions of the western CFT, which have a weak long-term geomorphic expression and thus, are expected to have a younger age.

The comparison between CFT and PQFS is suggestive of a tendency of the fault to simplify a major geometric complexity (Riedel shear arrangement) towards a straighter and mature trace that is presumably a mechanically more favorable setting for the fault to rupture. This evolution is in agreement with the results of analog deformation experiments, designed to evaluate the structural patterns that develop in sedimentary strata above a deep-seated strike-slip fault [54-57] (fig. 4). The structures developing as a result of increasing cumulative displacement are: 1) over-stepping, *en échelon* array of left-stepping synthetic Riedel shears; 2) some R-shears are rotated and few new R-shears appear at lower inclinations (α, fig. 4); 3) a second array of right-stepping synthetic shears (P-shears or Thrust-shears), that locally join or end up to the R-shears; 4) P-shears growth and linkage to R-shears, that form elongated shear lenses; 5) Y-shears, in a typical anastomosing pattern of a through-going wrench fault, parallel and superimposed on the deep-seated strike-slip faults [55].

Thus, we can conclude that: a) the PQFS and CFT are the superficial expression of the Düzce fault at depth; b) the PQFS and the CFT did not develop simultaneously but they represent different stages of evolution (i.e., early and mature stages, respectively); c) on the basis of the relationships between CFT and PQFS, the Düzce fault can be subdivided into two main sections the eastern and western ones approximately separated by the Cakirhaciibrahim village; d) the western section of the CFT is predominantly controlled by the PQFS arrangement and is related to persistent transtensional kinematics, and contains still immature E-W strands (incipient Y-shears, stage 4 in fig. 4); e) the eastern section is presently controlled by clear and mature E-W strands (Y-shears, stage 5 in fig. 4), accommodating most of the Düzce fault slip at the surface with the PQFS completely overcome.

3.4. The overall long-term morphological expression

Although with internal differences, the overall long-term morphological expression depicts the Düzce fault as a single and continue structural element, from the Karadere section to east of Kaynasli.

Because of the geometrical setting of the Düzce with respect to the Karadere fault section, that may be suggestive of a strict interaction between them, we widened the area of investigation to the west. We collected observations on the relationships among the Karadere restraining bend, the Düzce fault and the Düzce Basin. The Karadere section and the Düzce fault are two diverging strike-slip strands that are linked by a fault junction (*sensu* [50]). This geometrical array configures a releasing fault-wedge whose long-term morphological expression is represented by the wedge-shaped basin of the Golyaka area (fig. 2 and 5). Here, the vertical component of the movement strongly controls the drainage system. In fact, in the Düzce Basin, the streams arrangement has a centripetal pattern, converging to the present basin depocentre, the Efteni Lake (fig. 2). This has been migrating from the central part of the basin southwestward, shifting 12 km in ca. 2.5 My, with a velocity of about 4.8 mm/y [51] (fig. 2). The only stream that drains the Efteni Lake, flows northward and crosses orthogonally the Karadere restraining bend. This is responsible for the north-eastward transpressional motion and growth of a pressure ridge that comes into and deforms the Düzce Basin deposits, damming and pushing the north-flowing stream as testified by paleo-valleys and wind-gaps (spot 3 in fig. 2). For these reasons, only the westernmost part of the Düzce Basin in the Golyaka area, is the present-day fault-related floodplain. The northern part of the basin is no more active.

4. The interaction between the Düzce and Karadere fault sections

The right-lateral coseismic slip distribution at the surface and the overall long-term morphology suggest that the Düzce fault is a continuous fault segment that splays out from

the releasing junction with the Karadere section (fig. 2 and fig. 5). Although it exhibits such a continuity, we have defined a clear difference in the setting, structural evolution and fault related landscape of its eastern and western parts. The question is now to understand what can be the cause of this difference. The junction between the Karadere and Düzce faults represents a clear singularity in the geometrical arrangement in this part of the NAFZ. Under this light, we tested if the basin setting and landscape of the westernmost part of the Düzce Basin derive from the accumulation of repeated 1999-type earthquakes. For this purpose we compared the observed basin setting and topography with the coseismic deformation field.

We modeled the expected coseismic deformation field by using a standard dislocation code developed by Ward and Valensise [58]. To get a complete image of the fault related landscape, we introduced in the model not only the Düzce and Karadere 1999 fault segments but also Mudurnu 1967 and Mudurnu 1957 earthquake segments which may have also a role in shaping the study area (fig. 1). We assumed planar, rectangular faults, embedded in an elastic half-space with uniform slip. Slip during the most recent earthquakes on these faults (i.e. 1999, 1967, 1957) is considered characteristic [59]. The modeled fault parameters (fig. 5b and 5c), were derived from available coseismic seismological, geodetic and geological observations and are summarized in table 1.

From the resulting dislocation model we reconstructed two maps for the vertical and N-S component of surface deformation, respectively (fig. 5b and 5c). Obviously, modelling faults as boxes and assuming characteristic and uniform slip, without any tapering off at fault tip lines, are oversimplifications. Nevertheless, with exception for some minor mismatches (e.g. subsiding portion of the Karadere section hanging-wall) and discrepancies that may depend on inheritance from the previous compressional phases [27], the maps show how the repetition of earthquakes on the four modeled faults contributed in building up the present long-term landforms of the study area.

In particular figure 5 shows: 1) the uplift of the Almacik block; 2) the subsidence of the Akyazi basin; 3) the uplift of the northern part of the Düzce Basin with maxima located at the north-eastern tip of the Karadere fault; 4) subsidence of the Golyaka fault-wedge basin, in coincidence with the present active floodplain, with maxima at the western tip of the Düzce fault; 5) maximum N-S extensional component of the deformation across the western section of the Düzce fault.

Another outcome of this modeling is that the Düzce basin is not entirely fault-related and, as whole, it can not be considered an active pull-apart basin. The Golyaka fault-wedge area is experiencing a present-day important subsidence, whereas the north-western part of the Düzce basin is shrinking because of the transpressional deformation due to the Karadere restraining bend (fig. 5a and 5b).

Finally, a further indication derived from the test of the mechanical interaction between Karadere and Düzce faults shows that this interaction produces a zone across the western part of the Düzce fault with high extension normal to the fault. This translates to reduced normal stress in this part of the fault that can be seen as the cause for the difference between the two Düzce sections discussed in the previous chapter.

5. Comparing data from surface and depth

To understand if our observations at the surface contain some insights on the structure at depth, we compare the surface data discussed above with the Delouis et al. model of the 1999 coseismic slip distribution at depth (fig. 6; [24] but see also similar modelling from [40, 44, 45, 60, 61]). Interestingly, this comparison shows that the projection at depth of the boundary between the western and the eastern Düzce fault sections, we highlighted at the surface, coincides with an abrupt decrease of the slip distribution at depth. In fact, this boundary separates a portion of fault plane containing a

single asperity with two main patches of ca.8 m maximum slip to the east, and a portion with low slip generally not exceeding 2 m, to the west. However, the slip boundary (i.e. discontinuity) at depth does not coincide at the surface with a relevant change of strike-slip distribution but only with a different dip-slip distribution and a change in the arrangement of the structural pattern. In fact, the observed slip of the western Düzce fault section present maxima of 4.5 m at the surface, whereas, it does not exceed 2 m at depth. This inconsistency may be related to dynamical properties of the rupture.

A possible explanation for the difference between the two Düzce fault sections both at depth and surface can be found in the interaction Karadere-Düzce faults that, as discussed in the previous chapter, appears to result in a lower normal stress across the Düzce fault. This, on one side could be responsible for the premature stage of evolution of the western Düzce section at the surface (saw-tooth style, stage 4 in fig. 4) and, on the other, it could be responsible for the lack of asperities at depth.

Because the regional tectonic loading at the scale of the fault should be considered constant, the missing coseismic slip in the western section should be accommodated in a different way. Possibilities are: 1) microseismicity; 2) aseismic behaviour, with minor stress storage during the interseismic phase; 3) strain transfer to the eastern asperity as velocity-strengthening frictional afterslip [62] during the postseismic phase; 4) partitioning of the slip between the Karadere and western part of the Düzce fault; 5) concurrence of the above hypotheses.

6. Conclusions

On the basis of new results from aerial photo interpretation and field survey performed in the Düzce area, we have identified a Düzce 1999 coseismic fault trace (CFT) and Düzce Plio-Quaternary fault system (PQFS) (fig. 2). The first has a overall trajectory

ca. sub-parallel to the mean fault trend, whereas the second is composed of a Riedel system that is more complex than the CFT and involves a wider zone of deformation.

The comparison of the PQFS with the CFT provides the insights to understand how the fault arrangement has been evolving through time. The relatively simple, E-W trace of the CFT, represents the latest stage of the evolution of the fault (Y-shears, fig. 4) overcoming the geometrical complexities of the PQFS. The superimposition of the CFT on the PQFS is suggestive of a tendency of the fault to simplify its trace with time and to evolve from a complex structure towards a simple mature trace that appears to be a mechanically more favorable setting.

On the basis of the relations between the PQFS and CFT the Düzce fault can be subdivided into two sections (fig. 2): (a) the western section where the CFT follows mainly the saw-tooth trajectory of the PQFS and (b) the eastern section where the CFT cross-cuts the en-échelon pattern of the PQFS and is formed by mature E-W trending Y-shears. The eastern and western fault sections represent different stages of the evolution of the PQFS toward the CFT. The complex PQFS stage is already overcome in all the fault, but we can still see the fault in activity at the other three stages with increasing maturity: (1) the saw-tooth setting in the western CFT section (stage 4 in fig. 4) (2) the incipient Y-shears in the eastern part of the western section (spots e, f and g in fig 2) and (3) the Y-shears in the eastern section, parallel to the Düzce master fault that violated completely the organization of the PQFS (stage 5 in fig. 4).

The difference between the two Düzce sections appears to originate from the releasing junction the Düzce and Karadere faults. In fact, the mechanical interaction of these faults produces a zone of low normal stress across the western part of the Duzce fault (fig. 5) that may have delayed the evolution of the fault zone.

Interestingly, because (1) the difference between the two Duzce fault sections is not only at the surface but coincides with an important change in the 1999 slip distribution at

depth (fig. 6) and (2) the analysis of fault pattern, long-term landscape, and dislocation modeling, suggest that this difference is a permanent feature at the surface, we could hypothesize that also the difference of slip distribution at depth is a permanent feature. In this hypothesis, the low normal stress across the western Düzce fault becomes a permanent characteristic of that part of the fault and results in an unfavorable setting for hosting important asperities in this part of the fault also in the future.

The low normal stress in the western part of the Düzce fault originating from the Karadere-Düzce mechanical interaction may play a role also in the rupture propagation. According to studies on dynamics of the rupture, the dominant factor affecting rupture propagation beyond fault discontinuities (i.e. step-over, bend, double bend, fault junction) is normal stress rather than shear stress [6 and references therein]. When fluid pressure differentials are not able to act as barrier [2], a lower normal stress along the discontinuity favors the rupture propagation, but lowers its velocity and delays its triggering on the contiguous fault segment [47, 48]. Under this light, the Karadere-Düzce release fault junction could also have driven the delayed propagation of the August 17, 1999 Izmit rupture on the Düzce fault, which nucleated on the asperity of its eastern section three months later, on November 12, 1999.

One of the main outcome of this work is to highlight the potential of the geological and geomorphological analysis for imaging seismogenic sources also at depth and in shading light on their intermediate/long term behavior. This makes clear also the critical contribution that can derive from segmentation models for the prediction of future earthquake ruptures styles.

Acknowledgements

This research is supported by the European Commission Project *Relief*: Large earthquake faulting and implications for seismic hazard assessment in Europe: The Izmit-Düzce earthquake sequence of 1999, Turkey, Mw 7.4, 7.1, EVG1-CT-2002-00069.

References

[1] Segall, P., and D.D. Pollard (1980): Mechanics of discontinuous faults, *J. Geophys. Res.,* 85 (B8), 4337-4350.

[2] Sibson, R.H. (1985), Stopping of earthquake ruptures at dilational fault jogs, *Nature*, 316, 248-251.

[3] Barka A.A. and K. Kadinski-Cade (1988), Strike-slip fault geometry in Turkey and its influence on earthquake activity, *Tectonophysics*, *7*, 663-684.

[4] Wesnousky, S.G., (1988): Seismological and structural evolution of strike-slip faults, *Nature, 335*, 340-343.

[5] An, L.Y., (1997), Maximum link distance between strike-slip faults: Observations and constraints, *Pure and Applied Geophysics*, 150, 19-36.

[6] Kase, Y. and K. Kuge (2001), Rupture propagation beyond fault discontinuities: significance of fault strike and location, *Geophys. J. Int.*, 147, 330–342.

[7] Barka, A.A. (1992), The North Anatolian fault zone, *Annales Tectonicae*, *6*, 164-195.

[8] Şengör, A.M.C., O. Tüysüz, C. YImren, M. Sakýnç, H. Eyidogan, N. Görür, X. Le Pichon and C. Rangin (2005), The North Anatolian Fault: a new look, *Annu. Rev. Earth Planet. Sci.*, 33, 37-112.

[9] Reilinger, R.E., S.C. McClusky, M.B. Oral, W. King and M.N. Toksöz (1997), Global Positioning, System measurements of present-day crustal movements in the Arabian-Africa-Eurasia plate collision zone, *J. Geophy. Res.*, *102* (B5), 9983-9999.

[10] Reilinger, R.E., Toksöz, M.N., McClusky and A.A. Barka (2000), 1999 Izmit, Turkey Earthquake was no surprise, *GSA Today*, *10*, 1-6.

[11] Straub, C., H. G. Kahle, and C. Schindler (1997), GPS and geologic estimates of the tectonic activity in the Marmara Sea region, NW Anatolia, *J. Geophys. Res.*, *102* (B12), 27587-27601.

[12] McClusky, S.C., A. Balassanian, A.A. Barka, C. Demir and S. Ergintav (2000), Global positioning system constrain on plate kinematics and dynamics in the eastern Mediterranean and Caucasus, *J. Geophy. Res.* 105 (B3), 5695-5720.

[13] Kahle H. G., M. Cocard, Y. Peter, A. Geiger, R. Reilinger, S.C. McClusky, R. King, A. Barka and G. Veis, (1999), GPS-derived strain rate field within the boundary zones of the Eurasian, African, and Arabian Plates, *J. Geophy. Res*., 105 (B3), 23,353-23,370.

[14] Kahle H. G., M. Cocard, Y. Peter, A. Geiger, R. Reilinger, A. Barka and G. Veis (2000), GPS-derived strain rate field within the boundary zones of the Eurasian, African, and Arabian Plates, *J. Geophy. Res*., 105 (B3), 23,353-23,370.

[15] Tokay M. (1973), Kuzey Anadolu Fay Zonunun Gerede ile Ilgaz arasındaki kısmında jeolojik gözlemler. In *Kuzey Anadolu Fayi ve Deprem Kus¸ağı Simp., 29–31 Mart 1972, Ankara*, Tebliğler: M. T. A. Enst., Ankara, 12–29.

[16] Seymen, I. (1975). Kelkit Vadisi Kesiminde Kuzey Anadolu Fay Zonunun Tektonik Özelliği: Dr. Eng., Istanbul Tek. Üniv., Maden Fak., XIX+192 pp.+2 foldout maps.

[17] Barka, A.A., and P.L. Hancock (1984), Neotectonic deformation patterns in the convex-northwards arc of the North Anatolian fault zone, *J. Geol. Soc. London,* Spec. Pub., 17, 763-774.

[18] Hubert-Ferrari, A., R. Armijo, G. King, B. Meyer and A. Barka (2002), Morphology, displacement, and slip rates along the northern Anatolian Fault, Turkey, *J. Geophys. Res*., 107 (B10), 2235, doi:10.1029/2001JB000393, 33 pp.

[19] Ambraseys, N.N. (1970), Some characteristic features of the North Anatolian fault zone, *Tectonophysics*, *9*, 143-165.

[20] Ambraseys N.N. (2002), The seismic activity of the Marmara Sea region over the last 2000 years, *Seism. Soc. Am. Bull*., *92* (1), 1-18.

[21] Ambraseys N.N. and C.F. Finkel (1995), The seismicity of Turkey and adjacent areas: a historical review, 1500-1800, *Muhittin Salih Eren*, 240 pp., Istanbul.

[22] Akyüz, H.S., R.D. Hartleb, A.A. Barka, E. Altunel, G. Sunal, B. Meyer and R. Armijo (2002), Surface rupture and slip distribution of the 12 November 1999 Düzce earthquake (M7.1), North Anatolian Fault, Bolu, Turkey, *Seism. Soc. Am. Bull.*, *92* (1), 61-66.

[23] Lettis, W., J. Bachhuber, R. Witter, C. Brankman, C.E. Randolph, A. Barka, W.D. Page and A. Kaya (2002), Influence of releasing step-overs on surface fault rupture and fault segmentation: examples from the 17 August 1999 Izmit earthquake on the North Anatolian Fault, Turkey, *Seism. Soc. Am. Bull.*, *92* (1), 19-42.

[24] Delouis, B., D. Giardini and P. Lundgren, Düzce rupture model in *Database of Finite-Source Rupture Models*, Mai. P.M. Editor, Institute of Geophysics, ETH Zurich, Switzerland. (http://www.seismo.ethz.ch/srcmod).

[25] McKenzie, D.P. (1972), Active tectonics of the Mediterranean region, *Geophys. J. R. Astron. Soc., 30*, 109-185.

[26] Şengör, A.M.C. (1979), The North Anatolian transform fault: Its age, offset and tectonic significance. *J. Geol. Soc. London*, *136*, 269-282.

[27] Şengör, A.M.C, N. Görür and F. Şaroğlu (1985), Strike-slip faulting and related basin formation in zones of tectonic escape: Turkey as case study, in *Strike-slip Faulting and Basin Formation*, K.T. Biddle and N. Christie-Blick (Editors), Soc.Econ. Paleont. Min. Spec. Publ., 227-264

[28] Şaroğlu, F., Ö. Emre and İ. Kuşçu (1992), Active fault map of Turkey, General Directorate of Mineral Research and Exploration, Ankara.

[29] Ayhan, M.A., C. Demir, A. Kiliçoglu, I. Sanli, and S.M. Nakiboglu (1999), Crustal motion around the western segment of the north Anatolian fault zone: geodetic

measurements and geophysical interpretation, International Union of Geodesy and Geophysics (IUGG99), Birmingham, United Kingdom, 18-30 July.

[30] Ayhan, M.E., R. Burgmann, S. McClusky, O. Lenk, B. Aktug, E. Herece and R.E. Reilinger (2001), Kinematics of the Mw=7.2, 12 November 1999, Düzce, Turkey earthquake, *Geophys. Res. Let.*, 28 (2), 367-370.

[31] Canıtez N. and SB. Üçer (1967), A Catalogue of Focal Mechanism Diagrams for Turkey and Adjoining Areas. *˙ITÜ Maden Fak., Arz Fiziği Enst. Yayın* No. 25. 111 pp.

[32] Orgülü G. and M. Aktar (2001). Regional moment tensor inversion for strong aftershocks of the August 17, 1999 ˙Izmit earthquake (Mw= 7.4). *Geophys. Res. Lett.*, 28:371–74.

[33] Taymaz T, Jackson J, McKenzie D. 1991. Active tectonics of the north and central Aegean Sea, *Geophys. J. Int.*, 106, 433–90.

[34] Ambraseys, N.N. and A. Zatopek (1969), The Mudurnu valley, west Anatolia, Turkey, earthquake of 22 July 1967*Seism. Soc. Am. Bull.*, 59 (2), 521-589.

[35] Pinar, A., Y. Honkura and M. Kikuchi (1996), A rupture model for the 1967 Mudurnu Valley, Turkey earthquake and its implications for seismotectonics in the western part of the North Anatolian fault zone, *Geophys. Res. Lett.*, 23 (1), 29-32.

[36] Barka, A.A (1999), 17 August 1999 Izmit earthquake, *Science*, *285*, 1858-1859.

[37] Barka, A.A., H.S. Akyüz, E. Altunel, G. Sunal, Z. Çakir, A. Dikbas, B. Yerli, T. Rockwell, J. Dolan, R. Hartleb, T. Dawson, T. Fumal, R. Langridge, H. Stenner, S. Christofferson, A. Tucker, R. Armijo, B. Meyer, J. de Chabalier, W. Lettis, W. Page and J. Bachhuber (2000), The August 17, 1999 Izmit earthquake, M = 7.4, eastern Marmara region, Turkey; study of surface rupture and slip distribution, *The 1999 Izmit and Düzce earthquakes; preliminary results*, edited by A.A. Barka et al., pp. 15-30, Istanbul Technical University, Istanbul.

[38] Barka, A.A., H.S. Akyüz, and 18 others (2002), The surface rupture and slip distribution of the August 17, 1999 İzmit earthquake, M=7.4, North Anatolian Fault, *Seism. Soc. Am. Bull.*, *92* (1), 43-60.

[39] Muller, J.R., A. Aydin and F. Maerten (2003), Investigating the transition between the 1967 Mudurnu Valley and 1999 Izmit earthquakes along the North Anatolian fault with static stress changes, *Geophys. J. Int.*, *154*, 471-482.

[40] Utkucu M., S.S. Nalbant, J. McCloskey, S. Steacy and O. Alptekin, (2003), Slip distribution and stress changes associated with the 1999 November 12, Düzce (Turkey), *Geophys. J. Int.*, *153* (1), 229-241.

[41] Akyüz, H.S., A.A. Barka, E. Altunel, R.D. Hartleb, and G. Sunal (2000), Field observations and slip distribution of the November 12, 1999 Düzce earthquake (M=7.1), Bolu - Turkey, *The 1999 Izmit and Düzce earthquakes; preliminary results*, edited by A.A. Barka et al., pp. 63-70, Istanbul Technical University, Istanbul.

[42] Hartleb, R.D., J.F. Dolan, H.S. Akyüz, T. Dawson, A.Z. Turker, B. Yerli, T. Rockwell, E. Toraman, Z. Çakir, A. Dikbas and E. Altunel (2002), Surface rupture and slip distribution along the Karadere segment of the 17 August 1999 Izmit and the western section of the 12 November 1999 Düzce, Turkey, earthquakes, *Seism. Soc. Am. Bull.*, *92* (1), 67-78.

[43] Emre, Ö., Y. Awata and T. Duman (Eds.) (2003), Surface rupture associated with the 17 August 1999 Izmit earthquake. General Directorate of Mineral Research and Exploration, Ankara, Turkey, ISBN: 975-6595-53-1, pp. 29–271.

[44] Bürgmann, R., M.E. Ayhan, E.J. Fielding, T.J. Wright, S. McClusky, B. Aktug, C. Demir, O. Lenk and A. Turkezer (2002), Deformation during the 12 November 1999 Düzce, Turkey, Earthquake, from GPS and InSAR Data, *Seism. Soc. Am. Bull.*, *92* (1), 161–171.

[45] Çakir, Z., A. Barka, J.B. De Chabalier, R. Armijo and B. Meyer (2003a), Kinematics of the November 12, 1999 (Mw=7.2) Düzce earthquake deduced from SAR interferometry, *Turkish J. Earth Sci.*, *12*, 105-118.

[46] Aydin, A., and D. Kalafat (2002), Surface Ruptures of the 17 August and 12 November 1999 Izmit and Düzce Earthquakes in Northwestern Anatolia, Turkey: Their Tectonic and Kinematic Significance and the Associated Damage, *Seism. Soc. Am. Bull.*, *92* (1),. 95–106.

[47] Harris, R.A. and S.M. Day (1993), Dynamics of fault interaction: parallel strike-slip faults, *J. Geophys. Res.*, 98, 4461-4472.

[48] Harris, R.A. and S.M. Day (1999), Dynamic 3D simulations of earthquakes on en echelon faults, *Geophys. Res. Lett.*, 18, 893-896.

[49] Emre Ö., Erkal T., Tchepalyga A., Kazancı N., Keçer M., Ünay E. (1998), Doğu Marmara bölgesinin Neojen-Kuaternerdeki evrimi, *Maden Tetk. Arama Derg.*,120, 289–314.

[50] Christie-Blick, N. and K.T. Biddle (1985), Deformation and basin formation along strike-slip faults, in *Strike-slip Deformation, Basin Formation and Sedimentation*, K.T. Biddle and N. Christie-Blick (Editors), Soc.Econ. Paleont. Min. Spec. Publ.,1-34.

[51] Kazancı, N., Emre, Ö., Keçer, M. (2003), Filling pattern tectonically active Düzce basin, western NAF, Turkey. Abstracts, *International Workshop on the North Anatolian, East Anatolian and Dead Sea Fault Systems; Recent Progress in Tectonics and Palaeosismology* 31 August- 12 September 2003, METU and MTA, Ankara, Turkey, p. 72.

[52] Ben-Zion, Y., Z. Peng, D. Okaya, L. Seeber, J.G. Armbruster, N. Ozer, A.J. Michael, S. Baris and M. Aktar (2003), A shallow fault-zone structure illuminated by trapped waves in the Karadere-Düzce branch of the North Anatolian Fault, western Turkey, *Geophys. J. Int.*, *152*, 699-717.

[53] Peng, Z. and Y. Ben-Zion (2004), Systematic analysis of crustal anisotropy along the Karadere-Düzce branch of the North Anatolian Fault, *Geophys. J. Int.*, *159*, 253-274.

[54] Riedel, W. (1929), Zur mechanic geologischer brucherscheinungen, *Centralbl. f. Mineral.*, *Abt. B*, 354-368.

[55] Tchalenko, J. S. (1970), Similarities between shear zones of different magnitudes, *Geol. Soc. Am. Bull.*, *81* (6), 1625-1639.

[56] Wilcox, R.E., T.P. Harding, and D.R. Seely (1973), Basic Wrench Tectonics, *A.A.P.G. Bull.*, *57* (1), 74-96.

[57] Naylor, M.A., G. Mandl and C.H.K. Sijpesteijn (1986), Fault geometries in basement-induced wrench faulting under different initial stress states, *Journal of Structural Geology*, *8* (7), 737-752.

[58] Ward, S.N., G. Valensise (1989): Fault parameters and slip distribution of the 1915, Avezzano, Italy earthquake derived from geodetic observations, *Seism. Soc. Am. Bull.*, 79, 690-710.

[59] Schwartz, D.P. and K.J. Coppersmith 1984, Fault behavior and characteristic earthquakes; examples from the Wasatch and San Andreas fault zones, *J. Geophys. Res.*, 89 (B7), 5681-5698

[60] Birgören, G., H. Sekiguchi and K. Irikura (2004): Rupture model of the 1999 Düzce, Turkey, earthquake deduced from high and low frequency strong motion data, *Geophys. Res. Lett.,* 31, L05610, doi:10.1029/2003GL019194.

[61] Bouin, M.P., M. Bouchon, H. Karabulut and M. Aktar (2004), Rupture process of the 1999 November 12 Düzce (Turkey) earthquake deduced from strong motion and Global Positioning System measurements, *Geophys. J. Int.*, 159 (1), 207-211.

[62] Hearn, E.H., R. Bürgmann and R.E. Reilinger (2002), Dynamics of Izmit earthquake postseismic deformation and loading of the Düzce earthquake hypocenter, *Seism. Soc. Am. Bull.*, *92* (1), 172-193.

[63] Tibi, R., G. Bock, Y. Xia, M. Baumbach, H. Grosser, C Milkereit, S. Karakisa, S. Zümbül, R. Kind and J. Zschau (2001), Rupture processes of the 1999 August 17 Izmit and November 12 Düzce (Turkey) earthquakes, Geophys. J. Int., 144, F1-F7.

[64] Özalaybey, S., M. Ergin, M. Aktar, C. Tapırdamaz, F. Biçmen and A. Yörük (2002), The 1999 Izmit Earthquake Sequence in Turkey: Seismological and Tectonic Aspects, *Seism. Soc. Am. Bull.*, *92* (1), 376–386.

[65] Feigl, K.L., F. Sarti, H. Vadon, S. McClusky, S. Ergintav, P. Durand, R. Bürgmann, A. Rigo, D. Massonnet and Rob Reilinger (2002), Estimating slip distribution for the Izmit mainshock from coseismic GPS, ERS-1, RADARSAT, and SPOT measurements, *Seism. Soc. Am. Bull.*, 92 (1),138–160.

[66] Çakir, Z., J.B. de Chabalier, R. Armijo, B. Meyer, A. Barka and G. Peltzer (2003b): Coseismic and early post-seismic slip associated with the 1999 Izmit earthquake (Turkey), from SAR interferometry and tectonic field observations, *Geophys. J. Int.,* 155 (1), 93-110.

[67] Iio, Y., S. Horiuchi, Ş. Barış, C. Çelik, J. Kyomen, B. Üçer, Y. Honkura and A.M. Işıkara (2002), Aftershock Distribution in the Eastern Part of the Aftershock Region of the 1999 Izmit, Turkey, Earthquake, *Seism. Soc. Am. Bull.*, 92 (1), 411–417.

[68] Muller, J.R., and A. Aydin (2004), Rupture progression along discontinuous oblique fault sets: implications for the Karadere rupture segment of the 1999 Izmit earthquake, and future rupture in the Sea of Marmara,*Tectonophysics*, 391, 283–302.

[69] Canıtez, N, (1972), Source mechanism and rupture propagation in the Mudurnu Valley, Turkey, earthquake of July 22, 1967, *Pure and Applied Geophysics*, 93, 116-124.

[70] Barka, A.A. (1996), Slip distribution along the North Anatolian Fault associated with the large earthquakes of the period 1939 to 1967, *Seism. Soc. Am. Bull.*, *86* (5), 1238-1254.

[71] Stein, R.S., A.A. Barka, J.H. Dieterich (1997), Progressive failure on the North Anatolian Fault since 1939 by earthquake stress triggering, *Geophys. J. Int.*, 128 (3), .594-604.

[72] Herece, E., and E. Akay, (2003),1:100.000 geological maps of the North Anatolian Fault, *General Directorate of Mineral Research and Exploration*, Ankara, Appendix 3 and 4.

Captions

Table 1. Parameters of the fault models utilized for the elastic dislocation calculations: (1) on the basis of aftershocks distribution [34, 63, 64] and maximum depth for coseismic slip from GPS inversion [10] and GPS, InSAR and Spot data [24, 45, 65, 66]; (2) USGS; (3) on the basis of aftershocks distribution [52, 67] and surface geology [43]; (4) on the basis of static stress analysis [68] and surface geology [43]; (5) on the basis of focal mechanisms [25, 69] and surface geology [34, 70]; (6) on the basis of rupture models from geodetic [44, 45] seismological [60] and joint inversion analysis [24]; (7) on the basis of rupture models from geodetic analysis [10, 65, 66]; (8) from seismic moment estimations [35, 39, 71].

Figure 1. The 1999 Izmit and Düzce earthquakes. Epicentre location (stars) and focal mechanism solutions from Harvard CMT, surface ruptures traces from Akyuz et al. [41]. Inset: Simplified tectonic setting of the eastern Mediterranean and westward extrusion of the Anatolian plate.

Figure 2. Sketch of the relationships between 1999 ruptures (CFT) and long-term fault system (PQFS). Shaded relief based on digital elevation model (DEM, interpolated from 10 m contours and auxiliary 5 m contours of 1:25.000 scale topographic maps). Contour interval 100 m. Late Pliocene-Holocene continental deposits (compilation by 1:25.000 scale field survey and by Herece and Akay [72]) and main drainage features of the Düzce basin are reported. (see fig. 1 for location). Inset shows the strain ellipse related to the shear couple of the Düzce master fault (grey arrows), trend of structures related to its extensional and compressional components (black arrows) are reported.

Figure 3. Horizontal and vertical slip distribution along the CFT in the study area. Uncertainties have been evaluated by measuring minimum and maximum of the displacement and their range depends on the type of piercing point used.

Figure 4. Sequence of structures in the Riedel experiment. Grey dashed lines mark the cumulative offset. α indicates the inclination of shear in degrees with respect to general direction of movement. Histograms show cumulative amount of displacements on shears at each stage of the deformation [modified from 55].

Figure 5. a) Schematic structural map of the North Anatolian Fault studied by means of elastic dislocation model. The SW-NE striking Karadere section represents a restraining bend of the Izmit segment, that bifurcates and links to the westernmost part of the Düzce segment by a fault junction. The inset shows a simplified sketch of the fault junction between Karadere section and Düzce faults [modified from 50]. b) Vertical component of elastic dislocation modeled for the North Anatolian Fault array of the study area. The boxes correspond to the projection at the surface of the Düzce, Karadere and 1967 and 1957 Mudurnu fault planes (see text for details). Contour interval 0.1 m. c) N-S horizontal component of elastic dislocation (same fault array than -b- see text for details). Contour interval 0.2 m.

Figure 6. Block diagram showing the coseismic strike-slip distribution at depth of the Düzce rupture (at scale) for a comparison with the structures, morphology and coseismic strike and dip-slip distribution at the surface. Dashed white line indicates the boundary between the two Düzce fault sections. Hypocentre and epicentre of the mainshock are reported. [modified from 24].

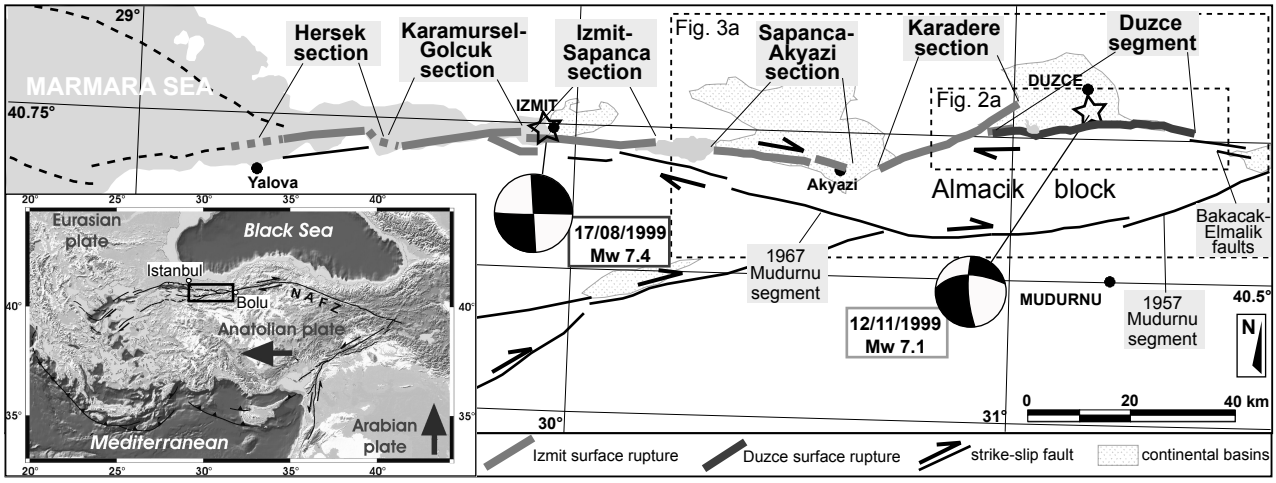
29°
MARMARA SEA
40.75°
Hersek section
Karamursel-Golcuk section
Izmit-Sapanca section
Fig. 3a
Sapanca-Akyazi section
Karadere section
Duzce segment
IZMIT
DUZCE
Fig. 2a
Yalova
Akyazi
Almacik block
Bakacak-Elmalik faults
17/08/1999 Mw 7.4
1967 Mudurnu segment
12/11/1999 Mw 7.1
MUDURNU
1957 Mudurnu segment
40.5°
N
0 20 40 km
30°
31°
Izmit surface rupture
Duzce surface rupture
strike-slip fault
continental basins
Eurasian plate
Black Sea
Istanbul
Bolu
NAFZ
Anatolian plate
Mediterranean
Arabian plate
20° 25° 30° 35° 40°
40°
35°

Fig. 1

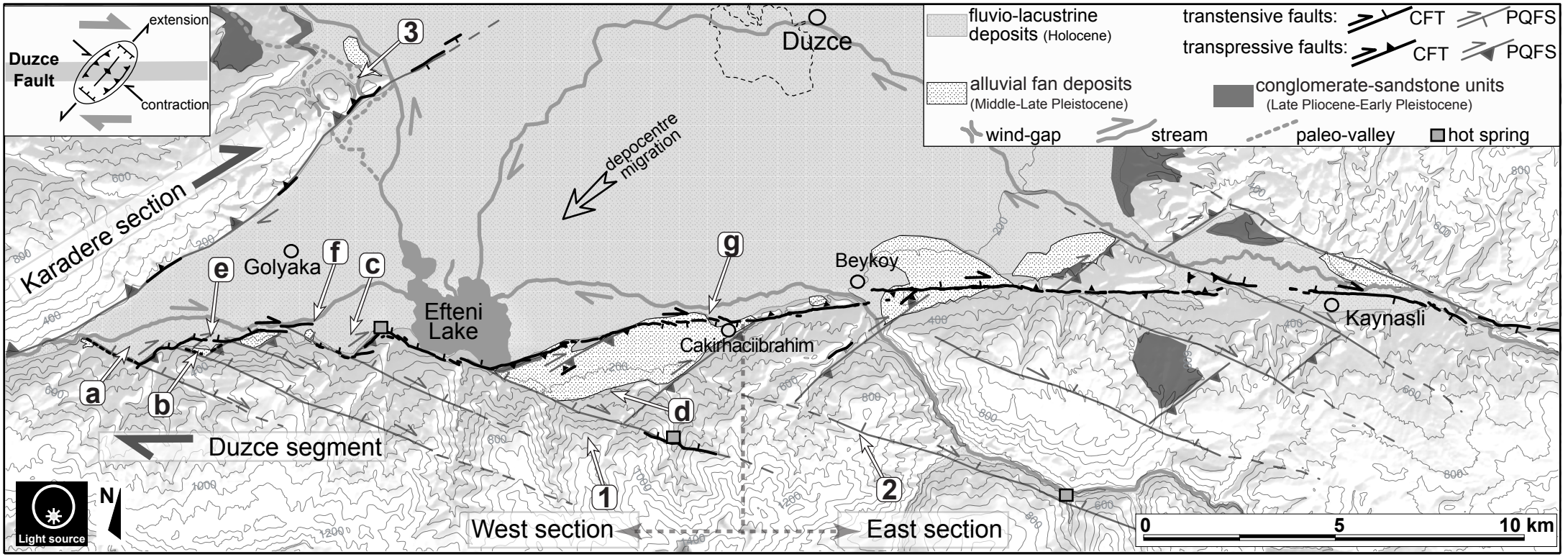
Duzce Fault
extension
contraction
Duzce
fluvio-lacustrine deposits (Holocene)
alluvial fan deposits (Middle-Late Pleistocene)
transtensive faults: CFT PQFS
transpressive faults: CFT PQFS
conglomerate-sandstone units (Late Pliocene-Early Pleistocene)
wind-gap
stream
paleo-valley
hot spring
depocentre migration
Karadere section
Golyaka
Efteni Lake
Cakirhaciibrahim
Beykoy
Kaynasli
Duzce segment
West section
East section
Light source
N
0 5 10 km
a
b
c
d
e
f
g
1
2
3

Fig. 2

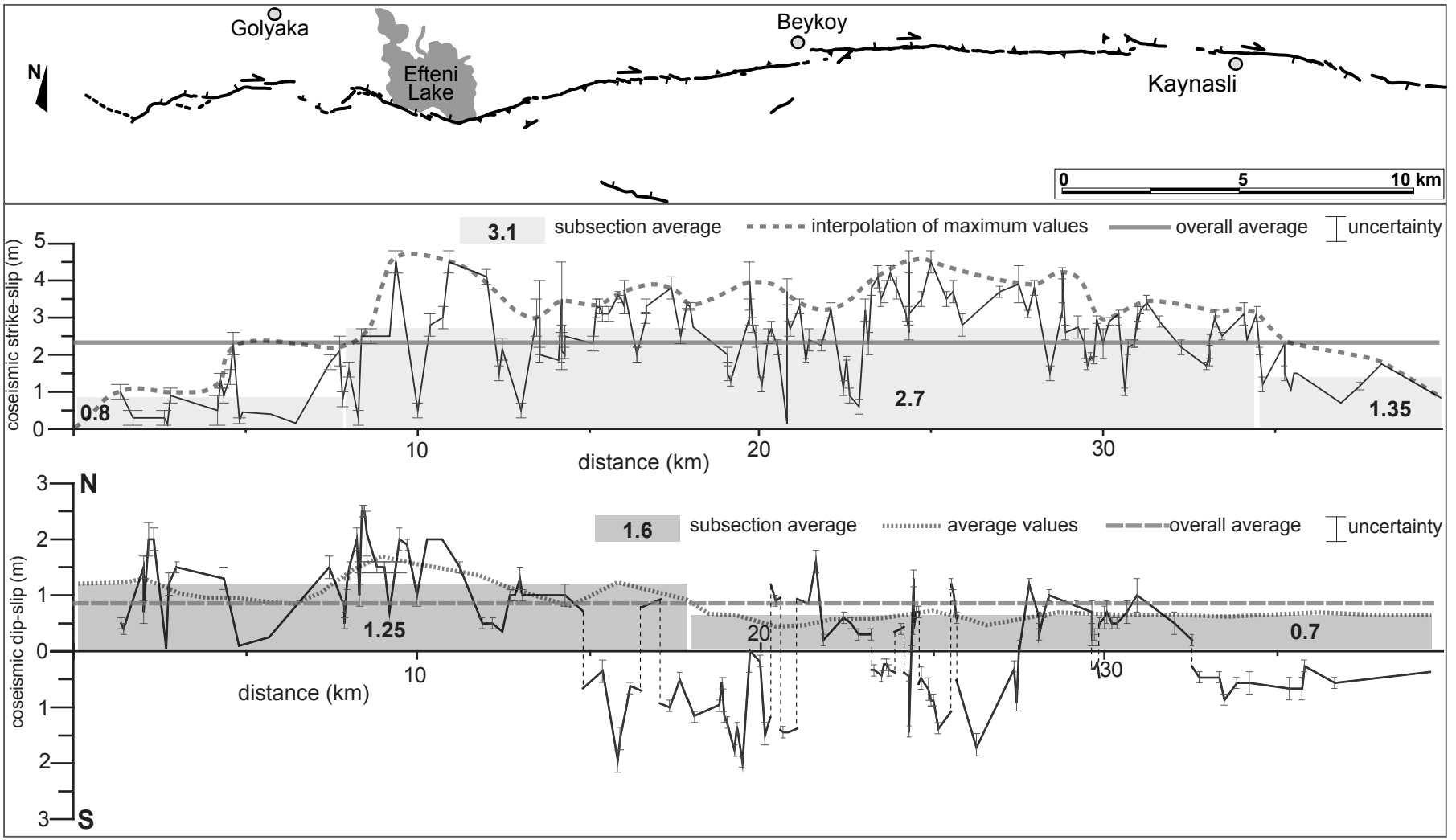
Golyaka
Efteni Lake
Beykoy
Kaynasli
N
0
5
10 km
3.1
subsection average
interpolation of maximum values
overall average
uncertainty
coseismic strike-slip (m)
0.8
2.7
1.35
distance (km)
N
1.6
subsection average
average values
overall average
uncertainty
coseismic dip-slip (m)
1.25
0.7
distance (km)
S

Fig. 3

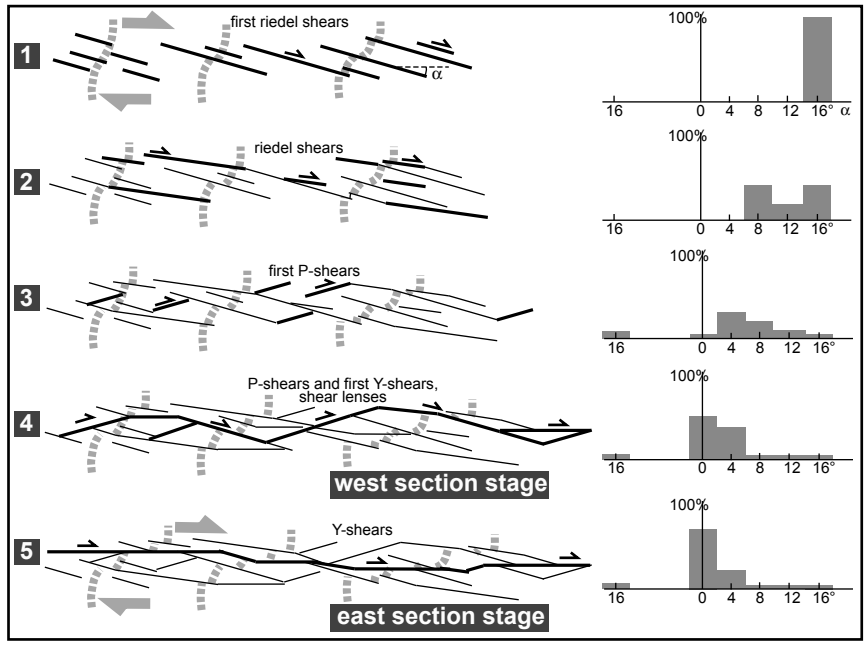
1
first riedel shears
α
100%
16 0 4 8 12 16° α
2
riedel shears
100%
16 0 4 8 12 16°
3
first P-shears
100%
16 0 4 8 12 16°
4
P-shears and first Y-shears,
shear lenses
west section stage
100%
16 0 4 8 12 16°
5
Y-shears
east section stage
100%
16 0 4 8 12 16°

Fig. 4

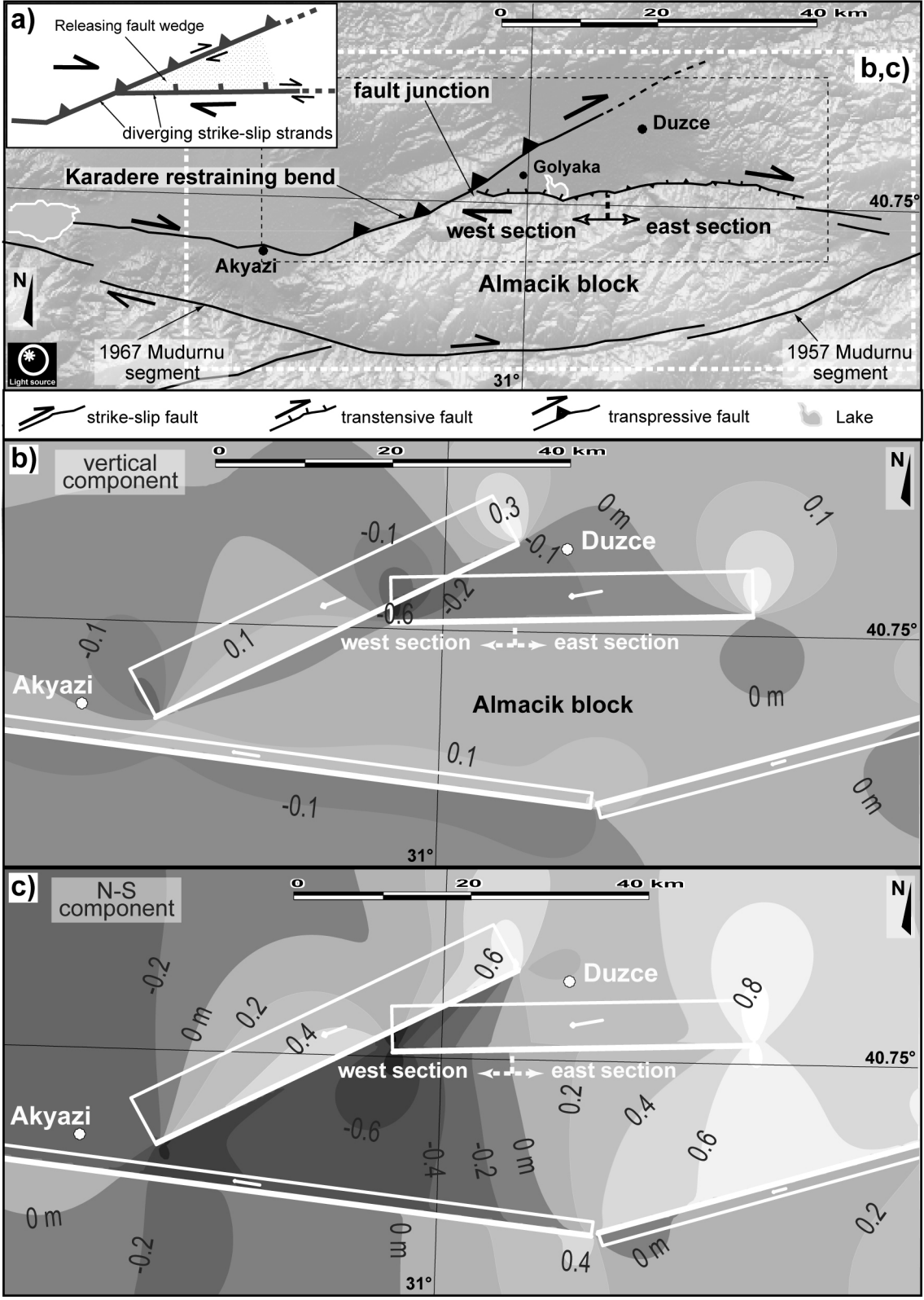
a)
Releasing fault wedge
diverging strike-slip strands
0
20
40 km
b,c)
fault junction
Duzce
Golyaka
Karadere restraining bend
40.75°
west section
east section
Akyazi
N
Almacik block
Light source
1967 Mudurnu segment
1957 Mudurnu segment
31°
strike-slip fault
transtensive fault
transpressive fault
Lake
b)
vertical component
0
20
40 km
N
0.3
0 m
0.1
-0.1
-0.1
Duzce
-0.6
-0.2
0.1
-0.1
40.75°
west section
east section
Akyazi
Almacik block
0 m
0.1
-0.1
0 m
31°
c)
N-S component
0
20
40 km
N
-0.2
0.6
Duzce
0.8
0 m
0.2
0.4
40.75°
west section
east section
Akyazi
0.2
0.4
-0.6
-0.4
-0.2
0 m
0.6
0 m
0 m
0.2
-0.2
0 m
0.4
0 m
31°

Fig. 5

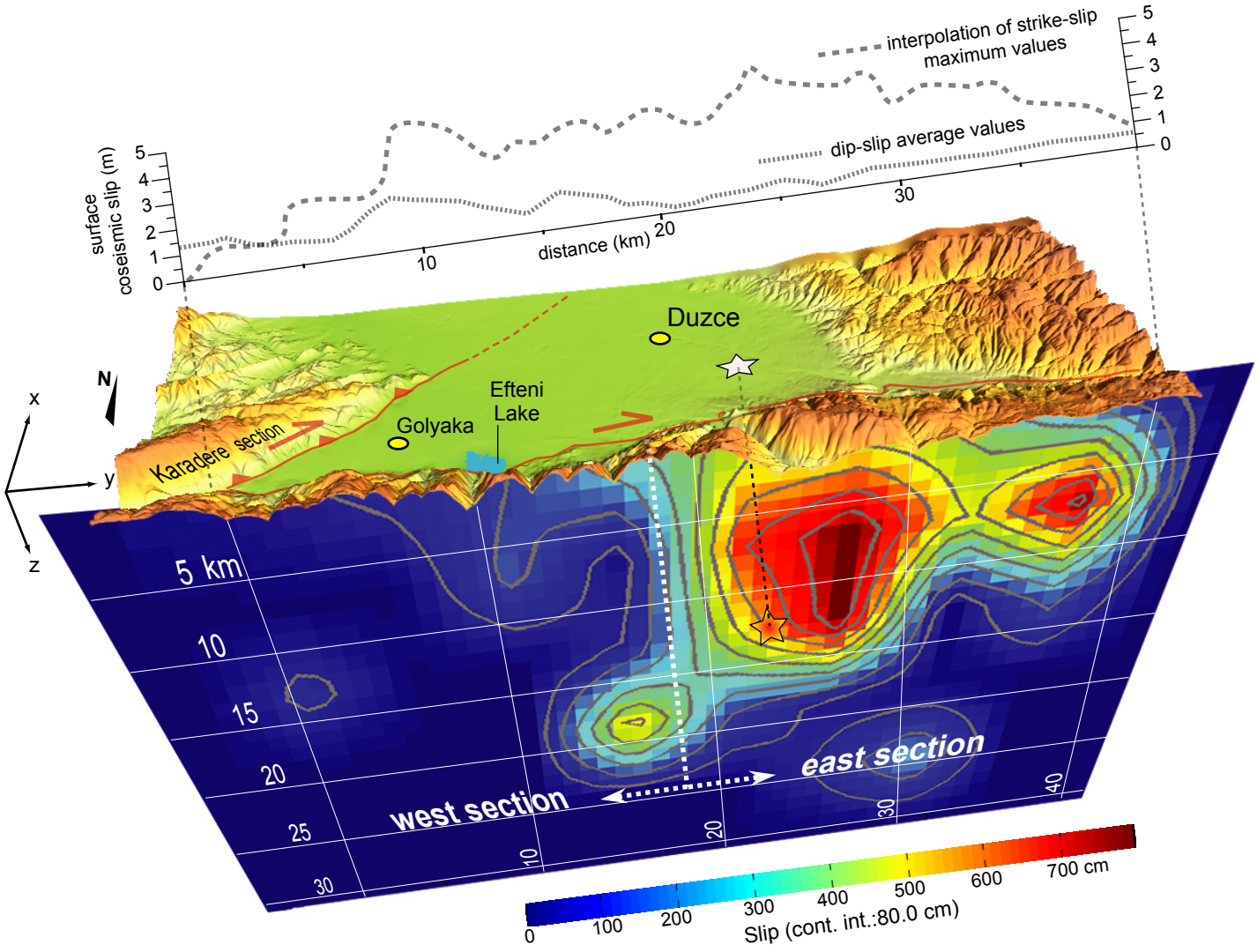
interpolation of strike-slip maximum values
dip-slip average values
surface coseismic slip (m)
distance (km)
Duzce
Efteni Lake
Golyaka
Karadere section
N
x
y
z
5 km
10
15
20
25
30
west section
east section
Slip (cont. int.:80.0 cm)
0
100
200
300
400
500
600
700 cm

Fig. 6

Table 1.

	Strike	Dip	Rake	slip	Lenght	Depth extent [1]
Düzce Fault	268° [2]	73° [2]	177° [2]	3.0 m [6]	40 km [2]	0-17 km
Karadere section	243° [3]	70° [3]	5° [4]	2.5 m [7]	45 km [3]	0-17 km
1967 Mudurnu segment	278° [5]	85° [5]	5° [5]	2.5 m [8]	80 km [5]	0-17 km
1957 Mudurnu segment	254° [5]	78° [5]	180° [5]	2.0 m [8]	40 km [5]	0-17 km